Investigation on Dimensionality Reduction methods for Tree-Crown Segmentation in Hyperspectral imagery using Segment Anything Model

Rewanth Ravindran[1 *], Yannick Treitz[1], Dorota Iwaszczuk[1]

[1] Technical University of Darmstadt, Dept. of Civil and Environmental Engineering Sciences,
Remote Sensing and Image Analysis, Darmstadt, Germany
(rewanth.ravindran, dorota.iwaszczuk)@tu-darmstadt.de, yannick.treitz@stud.tu-darmstadt.de

Keywords: hyperspectral remote sensing, dimensionality reduction, individual tree crown (ITC) delineation, SAM, factor analysis

Abstract

Forests play a vital role in global ecosystems, and accurate monitoring of tree crowns is essential for forest management and biodiversity conservation. This study investigates the use of hyperspectral imagery and dimensionality reduction methods for individual tree-crown (ITC) segmentation, a crucial task in forest monitoring. Traditional LiDAR-based methods are often expensive and computationally intensive, making hyperspectral imagery a promising alternative due to its data-richness. However, since most deep learning segmentation methods accept only 3-channel images, we adapt hyperspectral images from a benchmark dataset by applying dimensionality reduction techniques such as Principle Component Analysis (PCA), Factor Analysis, and Uniform Manifold Approximation and Projection (UMAP) to transform high-dimensional data into 3-channels, before performing segmentation using Segment Anything Model (SAM). The results show significant improvements over RGB imagery with dimensionality reduction methods, however the overall segmentation accuracy remains poor. With an average F1-score of 0.26, some methods achieved up-to 0.38 at specific sites. The results varied between sites due to different density and tree types in the image data. Factor Analysis and an approach with UMAP utilising vegetation indices produced the most promising results.

1. Introduction

Forests play a crucial role in biodiversity conservation and climate regulation. Effective forest monitoring requires up-to-date data on tree species, crown sizes, and forest structure. Remote sensing, especially hyperspectral imagery, has emerged as a key tool for capturing this information over large areas. A central challenge in forest monitoring is individual tree crown (ITC) segmentation, which aids in species classification, biomass estimation, and forest management (Ke and Quackenbush, 2011).

ITC segmentation research dates back to the 1980s, with early efforts focusing on detecting tree crown centres and using watershed segmentation. State-of-art methods of ITC delineation largely rely on the integration of LiDAR data and aerial imagery. Nonetheless, the acquisition of LiDAR data can be expensive and computationally intensive (Graves et al., 2023). As an alternative, multispectral and hyperspectral imagery (HSI) offer rich spectral information that can capture subtle differences in vegetation characteristics, yet the full potential of HSI remains under-explored (Ke and Quackenbush, 2011).

Hyperspectral remote sensing data differs from traditional RGB (red, green & blue channelled) imagery by offering a higher spectral resolution with hundreds of bands spanning a continuous spectrum across various wavelengths. Yet, processing this high-dimensional data presents challenges including increased computational complexity, overfitting, data sparsity and noise accumulation, and therefore it is frequently referred to as the "curse of dimensionality" (Powell, 2007). To address these challenges, dimensionality reduction techniques are employed to reduce the number of bands while preserving critical information. This also helps to compress data, improve computational efficiency, and facilitate visualisation (Li et al., 2022; Ruiz Hidalgo et al., 2021). Due to the continuous nature of HSI, adjacent spectral bands frequently exhibit high correlation, resulting in redundant information. Dimensionality reduction aims to eliminate this redundancy while preserving the intrinsic dimensionality of the data, which refers to the minimum number of dimensions required to represent the essential characteristics of the dataset (van der Maaten et al., 2007).

Different dimensionality reduction methods applied to HSI yield varying image characteristics, which significantly impact the accuracy of tree crown delineation. Therefore, selecting an appropriate dimensionality reduction method is crucial for improving segmentation results. However, only a few studies have addressed the optimal selection of dimensionality reduction methods for tree crown segmentation (Xi et al., 2021).

Segmentation plays a crucial role in remote sensing applications like urban planning and precision agriculture, but handling large data volumes remains a challenge, necessitating efficient processing techniques (Minaee et al., 2022). Additionally, availability of accurate annotations remains a major challenge for tree crowns compared to other segmentation tasks due to inherent complexity of tree crown structures in nature. This results in lack of adequate good quality training data, presenting difficulties in developing supervised deep learning algorithms for ITC segmentation (Steier et al., 2024).

Recent advances in computer vision have introduced novel approaches to unsupervised image segmentation in an attempt reduce these issues. One such promising tool is the Segment Anything Model (SAM) by MetaAI, which demonstrates notable results in general image segmentation applications without the need of training data (Kirillov et al., 2023; Wu and Osco, 2023). SAM represents a significant advancement in zero-shot segmentation, offering a foundation model that can be adapted

* Corresponding author

to a wide range of image segmentation tasks without requiring task-specific training (Kirillov et al., 2023). SAM's flexibility and computational efficiency make it particularly useful for high-resolution remote sensing applications (Osco et al., 2023). While SAM excels in 3-channelled RGB image segmentation, integrating it with multi-channel data such as HSI remains an active research area (Osco et al., 2023).

Our contribution: To address these research gaps, we propose the use of dimensionality reduction as a method to aid hyperspectral band-reduction for usability with SAM. By using the zero-shot principle based SAM, we also address challenges in developing a segmentation algorithm without the availability of adequate training data. The aim of the study is to compare various dimensionality reduction methods in order to find the optimal method resulting in the best segmentation performance using SAM. We assess the methods by using a benchmark dataset that contains multiple images from different forest sites with varying tree types and densities. We particularly focus on the effectiveness of the approach in answering the following research questions:

1. How does each dimensionality reduction method perform for the different forest type and density?
2. Does the high dimensionality of hyperspectral data provide additional latent spectral information that is useful for more accurate ITC segmentation?

The evaluation will determine whether reduced hyperspectral data offer clear advantages in terms of accuracy and segmentation performance. Through this, the study will investigate whether the dimensionality-reduced hyperspectral data provides meaningful enhancements compared to RGB or multispectral data, ultimately assessing its suitability for advancing tree crown delineation techniques.

2. Preliminaries

In this section, key dimensionality reduction (DR) methods for hyperspectral image segmentation considered in this work are outlined below. DR methods are categorised as supervised or unsupervised, with the latter not requiring labelled data (Li et al., 2022). Given the zero-shot segmentation nature of SAM, this study focuses on unsupervised methods, further divided into linear and non-linear approaches (van der Maaten et al., 2007).

2.1 Linear Dimensionality Reduction Methods

Linear dimensionality reduction techniques are particularly effective for datasets with intrinsic linear structures that can be captured by linear equations. However, they fail to adequately represent non-linear relationships present in real-world data, potentially missing important underlying structures (van der Maaten et al., 2007).

Principal Component Analysis (PCA) is a classical, widely used linear dimensionality reduction technique. PCA projects data onto orthogonal axes (principal components) ordered by variance. The initial components capture most of the variance, while later ones often represent noise (Li et al., 2022). **Factor Analysis (FA)** is another linear method that identifies latent variables explaining observed correlations, distinguishing between common and unique variances for more nuanced data representation (Yong and Pearce, 2013).

2.2 Non-linear Dimensionality Reduction Methods

Non-linear DR methods capture complex relationships within data but are more computationally demanding and sensitive to parameters (Khodr and Younes, 2011).

Independent Component Analysis (ICA) finds independent components, useful for hyperspectral unmixing but can produce noisier outputs than PCA (Lennon et al., 2001). **Multidimensional Scaling (MDS)** maps data into a space preserving distances between points, effective for non-linear datasets (Saeed et al., 2018). **Non-negative Matrix Factorization (NMF)** decomposes data into interpretable non-negative matrices, applied in hyperspectral unmixing (Wen et al., 2016). **t-Distributed Stochastic Neighbor Embedding (t-SNE)** preserves local data similarities for visualizations but struggles with high intrinsic dimensionality (Hinton and Roweis, 2002). **Uniform Manifold Approximation and Projection (UMAP)** balances local and global structure preservation with efficient processing, making it suitable for diverse high-dimensional data types (McInnes et al., 2020; Li et al., 2022).

3. Method

Our method was designed to assess how various dimensionality reduction techniques can improve tree crown segmentation. In the first section we discuss the different approaches to the dimensionality reduction methods employed in this study. This is followed by segmentation of the resultant 3-channel images from the previous step using SAM. Finally the eligible segmented results are filtered for evaluation against annotated data. The methodology is illustrated in Figure 1).

3.1 Dimensionality Reduction Approaches

Dimensionality reduction was performed using the Python Scikit-learn library (Pedregosa et al., 2011), which offers several established methods, including PCA, FastICA, MDS, NMF, t-SNE, and Factor Analysis. The UMAP method was utilised through the UMAP library (McInnes et al., 2020). While most dimensionality reduction methods offer parameter tuning, default values were used according to the respective documentation.

3.1.1 Local, Semi-Global and Global approaches The study tested various dimensionality reduction methods to determine the most functional and stable approach. To ensure comparability between different approaches, each method was applied at three different levels: local (for individual plots), semi-global (for all plots within a given site), and global (for all test sites). This approach tests the transferability of a specific method to different forest characteristics in the hyperspectral dataset, as a single image-based method might not capture all classes in the entire dataset.

For the local approach, PCA, t-SNE, ICA, NMF, MDS, FA, and UMAP methods were applied independently to each plot, reducing the hyperspectral data from 426 channels to three channels before segmentation. Each image consists of 1600 pixels (40x40 pixels) following this process. In the semi-global approach, the images were combined side-by-side into a composite image for each test site, with dimensionality reduction subsequently applied to this composite. Afterwards, the composite was split back into individual images. Methods PCA,

SiteID	Site Name	State	No. of Annotated Crowns	Ecosystem	Assigned Classification
ABBY	Abby Road	WA	160	Temperate rainforest	Moderate Coniferous
BART	Bartlett Experimental Forest	NH	93	Northern hardwood forest	Dense Broadleaf
BLAN	Blandy Experimental Farm	VA	73	Temperate deciduous forest	Dense Broadleaf
BONA	Caribou-Poker Creeks Research Watershed	AK	255	Boreal forest	Dense Coniferous
CLBJ	Lyndon B. Johnson National Grassland	TX	116	Temperate grassland	Sparse Trees
DELA	Dead Lake	AL	87	Deciduous forest and wetlands	Dense Broadleaf
DSNY	Disney Wilderness Preserve	FL	87	Wetlands and pine flatwoods	Sparse Trees
HARV	Harvard Forest	MA	117	Temperate deciduous forest	Dense Broadleaf
JERC	The Jones Center At Ichauway	GA	101	Longleaf pine forest and wetlands	Moderate Deciduous
LENO	Lenoir Landing	AL	75	Bottomland hardwood forest and wetlands	Dense Broadleaf
MLBS	Mountain Lake Biological Station	VA	481	Mixed hardwood forest	Dense Broadleaf
NIWO	Niwot Ridge	CO	1777	Alpine tundra and subalpine forest	Moderate Coniferous
OSBS	Ordway-Swisher Biological Station	FL	497	Pine flatwoods and wetlands	Moderate Deciduous
SCBI	Smithsonian Conservation Biology Institute	VA	73	Mixed deciduous forest	Dense Broadleaf
SERC	Smithsonian Environmental Research Center	MD	94	Tidal marshes and forest	Dense Broadleaf
SJER	San Joaquin Experimental Range	CA	422	Oak savanna and grassland	Sparse Trees
SOAP	Soaproot Saddle	CA	114	Mixed conifer forest	Moderate Coniferous
TALL	Talladega National Forest	AL	92	Mixed pine and hardwood forest	Dense Broadleaf
TEAK	Lower Teakettle	CA	1468	Mixed conifer forest	Moderate Coniferous
UNDE	University of Notre Dame Environmental Research Center	MI	186	Northern hardwood forest	Dense Broadleaf
WREF	Wind River Experimental Forest	WA	178	Temperate rainforest	Dense Coniferous

Table 1. Site information with updated image-segmented crowns, ecosystem types, and classification (Weinstein et al., 2020)

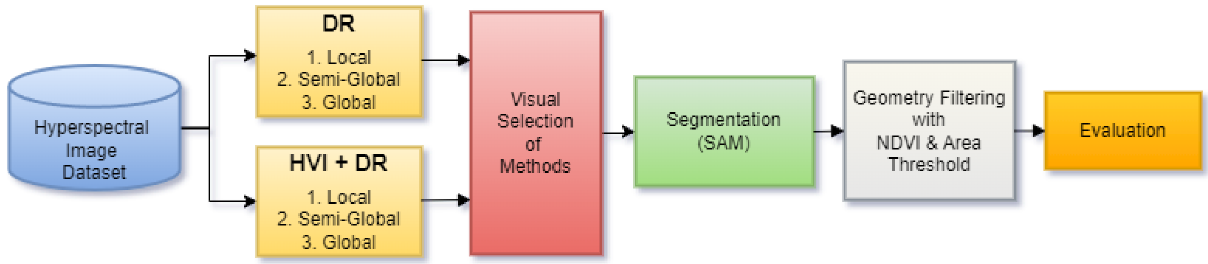

Figure 1. Flowchart of the Method, with main steps being dimensionality reduction (DR) of hyperspectral imagery and hyperspectral vegetation indices (HVI). Segmentation is performed with Segment Anything (SAM).

ICA, FA, and UMAP were included in this approach, but excluded MDS, NMF, and t-SNE due to the computational complexity and based on visual evaluation detailed in Section 4.2. The semi-global approach aims to reduce noise while sacrificing some local variation. The global approach involved reducing all plots simultaneously, using the same reduction methods as in the semi-global approach. This approach includes diverse surface types and spectral signatures, intending to further reduce noise at the expense of even more local detail compared to the local and semi-global approaches.

3.1.2 Dimensionality Reduction with Vegetation Indices

Vegetation indices (VIs) are well-established tools for quantifying vegetation cover and health based on plants' spectral characteristics (Xue and Su, 2017) and widely used in agriculture, forestry, and environmental monitoring. VIs combined with Principal Component Analysis (PCA) can be used for individual tree crown (ITC) delineation to significantly increase segmentation accuracy (Maschler et al., 2018).

In our approach, we computed seven commonly used vegetation indices (Table 2) and applied dimensionality reduction techniques to extract the most relevant information for segmentation. Because these indices were developed using multispectral data, we averaged over close hyperspectral bands to determine hyperspectral vegetation indices (HVI). Next, these seven single-channel vegetation indices were stacked into a seven-channel image. The stack was then reduced to three channels using PCA, FA, and UMAP. These three reduction methods showed promising results in preliminary studies. Additionally, the semi-global and global approaches were used also with the HVI imagery using FA, PCA, and UMAP methods, followed by the segmentation process.

Finally, to evaluate the benefits of hyperspectral data over conventional RGB imagery, we run our method with hyperspactral and high-resolution RGB images from the dataset. This allows us to assess any bias in segmentation using SAM, as the model was primarily trained on RGB data. To ensure a fair comparison, the RGB images were down-sampled from 0.1 meters to 1 meter resolution to match the hyperspectral image resolution.

3.2 Segmentation using SAM

Segment Anything Model (SAM) was chosen for the segmentation task for its ability to perform instance segmentation across diverse datasets with minimal manual intervention (Kirillov et al., 2023). The model was used in its default configuration, generating segmentation masks for each plot. Since SAM is designed for RGB data, 3-channel imagery was necessary. The dimensionality-reduced hyperspectral images, as explained in the previous section served as inputs for SAM.

Segmentation was performed using a version of SAM suitable for remote sensing datasets called GeoSAM (Wu and Osco, 2023). GeoSAM segmented each image into multiple masks representing different objects, and then each mask was saved as TIF files. These masks served as base for further tree crown segmentation filtering objects by size and spectral properties. A tree threshold was set from 4 m² to 200 m² to discard background and objects sizes unrealistic to represent trees. Additionally, objects below an Normalized Difference Vegetation Index (NDVI) value of 0.4 were excluded, representing non-vegetation objects, following the approach byMarconi et al. (2019).

3.3 Evaluation

The filtered geometries from the segmentation results were enclosed by bounding boxes and saved as rectangles in a CSV file for each plot. These files were later used for evaluation with

This contribution has been peer-reviewed. The double-blind peer-review was conducted on the basis of the full paper.
https://doi.org/10.5194/isprs-annals-X-G-2025-705-2025

Index	Full Name	Formula	Reference
NDVI	Normalized Difference Vegetation Index	$\frac{NIR-RED}{NIR+RED}$	Rouse et al. (1973)
EVI	Enhanced Vegetation Index	$2.5 \times \frac{NIR-RED}{NIR+6\times RED-7.5\times BLUE+1}$	Huete et al. (1999)
LAI	Leaf Area Index	$3.618 \times (EVI - 0.118)$	Boegh et al. (2002)
RENDVI	Red Edge NDVI	$\frac{NIR-RE}{NIR+RE}$	Gitelson and Merzlyak (1994)
CCCI	Canopy Chlorophyll Content Index	$\frac{RENDVI-min(RENDVI)}{max(RENDVI)-min(RENDVI)}$	Li et al. (2014)
SAVI	Soil Adjusted Vegetation Index	$\frac{NIR-RED}{NIR+RED+L} \times (1+L), L = 0.5$	Huete (1988)
NDWI	Normalized Difference Water Index	$\frac{NIR-SWIR}{NIR+SWIR}$	McFeeters (1996)

Table 2. List of implemented Vegetation Indices (NIR- Near Infrared band; RE- Red Edge; SWIR - Shortwave Infrared)

the NEONTreeEvaluation package in R. Using this package, precision and recall were calculated, to generate F1-score as the primary evaluation metrics following Marconi et al. (2019). Further, a bounding box was classified as positive if its Intersection over Union (IoU) exceeded 0.4.

4. EXPERIMENTS AND RESULTS

4.1 Dataset

The benchmark dataset utilised in this study is designed to evaluate the performance of tree delineation algorithms (Weinstein et al., 2020) and provided by the National Ecological Observatory Network (NEON). The data includes RGB data and hyperspectral data acquired using aerial imagery, at 0.1 m and 1 m resolutions respectively. Our study does not use the included LiDAR data, and the RGB data is used solely for comparative purposes. The benchmark also offers evaluation data, comprising totally over 6,000 image-annotated crowns, with multiple plots per site. The crowns were manually annotated by a single observer based on the dataset's RGB images. The 21 chosen test sites for this study reach from Florida to Alaska, encompassing forests dominated by conifers, broadleaves, or a combination of both (see Table 1). In total, 192 annotated hyperspectral images, each covering 40m x 40m plots from the 21 sites, were used.

4.2 Dimensionality Reduction Outcomes

The dimensionality reduction (DR) results varied considerably by method and plot characteristics. With **local DR** methods The performance of DR methods varied significantly depending on the specific plot and forest density. Plots with isolated trees (e.g. TEAK and SJER) performed well across all methods, while dense forest plots exhibited substantial noise in many cases. Methods such as t-SNE, PCA, UMAP, MDS, and ICA frequently produced noisy results, with 50% of the images containing minimal usable information. NMF also produced noisy results for some plots, often generating single-colour images. FA and HVI-based methods were notably more resistant to noise, yielding clearer results (Figure 2).

Semi-global approaches generally produced less noisy images compared to the local approach, although some methods, such as UMAP, ICA, and PCA, still struggled with noise in many plots (Figure 3). However, as noise reduced, object distinction suffered, with some images becoming almost monochromatic. FA and HVI-based methods performed best, with the clearest object separations. **Global DR approaches** resulted in the least noise across most methods, particularly for PCA and ICA (Figure 4). However, this came at the cost of reduced object differentiation, with many images appearing as single-colour or two-tone, complicating segmentation. FA and HVI-based methods maintained good performance in reducing noise, but even they experienced diminished object separability in the global approach. The final DR methods selected for segmentation were based on a visual evaluation, in order to manage computational costs effectively, which are as follows:

- FA applied to HSI locally and semi-globally
- FA, PCA, and UMAP applied to HVIs locally
- FA and UMAP applied to HVIs semi-globally
- RGB images (downscaled to match HSI resolution)

4.3 Segmentation Results and Performance Analysis

The segmentation results, shown in Figure 6, demonstrated that SAM performed well for high-contrast objects but faced limitations in dense forest plots, where objects were often merged into large "background geometries." NDVI-based filtering effectively excluded non-vegetation but sometimes retained non-tree vegetation, such as bushes or grass. Shadow segmentation was an issue in specific DR methods, leading to false positives.

Evaluation with the NEON-Tree-Evaluation package indicated F1 scores ranging from 0.236 to 0.274 for most DR methods, with RGB images showing lower performance (F1 score of 0.156). The best outcomes were observed with local FA and HVI-based DR methods applied semi-globally. Segmented and filtered bounding box counts varied, from approximately 2550 for RGB images to nearly 5000 in total for local HVI-UMAP. Performance also depended on test site characteristics; DSNY, WREF, BONA, and MLBS achieved the highest F1 scores, whereas NIWO, SERC, LENO, and ABBY performed the worst. An average IoU of 0.233 for FA highlighted it as the best-performing DR method overall. Detailed metrics and site-specific evaluations are provided in Table 3.

5. DISCUSSION

5.1 Dimensionality Reduction

The results of the dimensionality reduction process were visually assessed, revealing significant variation across different methods and test sites. For tree crown delineation, an effective DR method should allow clear separation of trees from the background and other objects. The most common issues encountered during DR were the prevalence of noise and the dominance of shadows in certain methods.

https://doi.org/10.5194/isprs-annals-X-G-2025-705-2025 |

Site	FA local	FA semi global	HVI FA local	HVI FA semi-global	HVI PCA local	HVI UMAP local	HVI UMAP semi-global	RGB	Average
Average:	0.274	0.267	0.266	0.272	0.244	0.263	0.236	0.156	0.261
ABBY	0.111	0.131	0.065	0.040	0.093	0.113	0.099	0.052	0.095
BART	0.000	0.035	0.182	0.192	0.164	**0.284**	**0.296**	0.091	0.169
BLAN	**0.357**	**0.259**	0.220	0.160	0.128	0.242	0.214	0.023	0.229
BONA	**0.337**	**0.365**	0.202	**0.303**	0.160	**0.327**	**0.276**	0.132	**0.286**
CLBJ	0.091	0.062	0.149	0.218	0.133	**0.280**	**0.275**	0.013	0.173
DELA	**0.276**	**0.397**	0.030	0.071	0.165	0.212	0.130	0.143	0.188
DSNY	**0.380**	**0.310**	**0.398**	0.247	0.248	**0.358**	**0.315**	**0.384**	**0.324**
HARV	**0.296**	**0.333**	0.162	0.208	0.151	0.212	0.140	0.040	0.218
JERC	**0.268**	0.218	0.144	0.171	0.107	0.244	**0.260**	0.055	0.205
LENO	0.111	0.142	0.037	0.063	0.081	0.110	0.083	0.000	0.092
MLBS	**0.272**	**0.251**	0.194	0.217	0.223	**0.281**	**0.293**	0.042	**0.251**
NIWO	0.072	0.068	0.075	0.079	0.079	0.086	0.068	0.048	0.076
OSBS	**0.257**	**0.298**	0.232	**0.269**	**0.287**	0.236	0.138	0.146	0.247
SCBI	0.076	0.058	0.132	0.135	0.112	0.210	0.215	0.059	0.135
SERC	0.063	0.084	0.051	0.019	0.031	0.186	0.144	0.034	0.087
SJER	0.208	0.213	**0.251**	**0.257**	0.207	0.207	0.213	0.131	0.224
SOAP	0.172	0.081	0.103	0.231	0.094	0.126	0.149	0.054	0.138
TALL	0.000	0.000	0.055	0.052	0.140	0.235	0.157	0.048	0.101
TEAK	0.219	0.217	**0.256**	**0.260**	0.242	**0.245**	0.137	0.147	0.227
UNDE	0.167	0.139	0.172	0.119	0.160	**0.282**	0.177	0.146	0.179
WREF	**0.415**	**0.374**	0.227	0.235	0.201	**0.309**	**0.285**	0.202	**0.298**

Table 3. F1 scores of various methods by site, with the best values (F1 score higher than 0.250) highlighted in bold

5.1.1 Noise Problem and its Impact

Noise was most pronounced in dense vegetation plots, while plots with distinct objects showed better differentiation across DR methods. Although semi-global and global approaches reduced noise, the global approach compromised object distinction due to increased pixel volume. This indicates that an optimal balance between local and global DR may enhance outcomes, with parameter tuning in methods such as UMAP and Isomap potentially improving the balance of local and global structures (Silva and Tenenbaum, 2002; McInnes et al., 2020).

Noise issues were particularly severe for UMAP, ICA, MDS, PCA and t-SNE, aligning with findings that outliers can degrade local DR performance, suggesting the need for preprocessing (van der Maaten et al., 2007). FA, NMF, and HVI-based methods showed greater noise resilience, though NMF occasionally produced noisy results. The reduced noise seen in semi-global and global approaches, especially with PCA and ICA, suggests that while scaling helps, it may reduce local detail.

5.1.2 Shadow Problem

Another prominent issue was the handling of shadows. Shadows have distinct spectral signatures compared to illuminated areas, and many DR methods accentuated these shadows, sometimes more than the trees themselves (Figure 6), thus shadows dominate in non-HVI-based methods, complicating the segmentation process. As shadows meet the NDVI threshold for soil vegetation, they are often retained in the final geometries, resulting in two segmented objects: the tree and its shadow.

HVI-based methods were particularly effective in mitigating the shadow problem, as their use of spectral ratios helped minimise the prominence of shadows (Figure 7). UMAP's use of the ”cosine” metric further addressed the issue, reducing the shadow's influence compared to the ”Euclidean” metric, as shown in Figure 8. However, UMAP continued to produce noisy results across most plots, indicating that parameter tuning, such as exploring alternative distance measures, may be necessary (Keshava, 2004).

5.2 Segmentation Results

The segmentation results revealed that GeoSAM performed well on high-contrast images with few distinct objects (Figure 5). However, in denser forests or low-contrast images, the segmentation process often failed to distinguish between objects, leading to over or under-segmentation.

Oversegmentation was most prevalent in the local HVI_UMAP method (Figure 5), which produced the highest recall(0.312) but a below-average precision score (0.227). In contrast, undersegmentation was observed across most DR other methods except HVI_UMAP, where multiple distinct objects were often merged with the background, especially in dense forests. Adjusting contrast and saturation in the DR results or tweaking SAM parameters could improve segmentation performance.

The geometry filtering process worked well but encountered some issues with incorrectly including non-tree vegetation and incorrectly excluding trees. The inclusion of bushes or grass was attributed to the filtering thresholds based on area and NDVI. Incorporating tree-specific vegetation indices or height data from LiDAR could enhance filtering accuracy. Conversely, annotated dead or dry trees were often excluded due to their blending with the background or failing to meet the NDVI threshold. This issue could be addressed by developing indices specifically tailored to detect deadwood or incorporating additional spectral information.

5.3 Evaluation of Segmentation Results

The average evaluation results were similar across different DR methods. No clear pattern has emerged predicting the performance of the methods (Table 3). This is further complicated due to factors like forest density or tree species. Another reason may be the small sample size, as the majority of sites have fewer than five evaluation plots. Notably, the best results found in TEAK and DSNY sites, which are characterised by single trees on rocky terrain, making segmentation and filtering easier. This highlights the potential for urban tree detection when similar image characteristics are present.

https://doi.org/10.5194/isprs-annals-X-G-2025-705-2025 | © Author(s) 2025. CC BY 4.0 License.

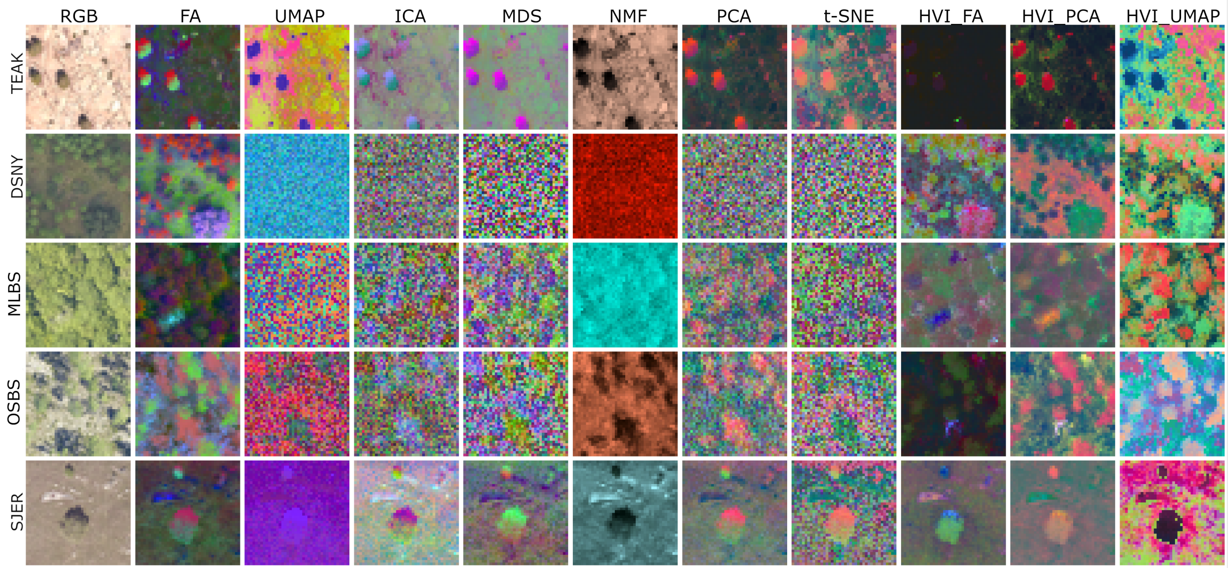

Figure 2. Dimensionality Reduction results using local approach of five example plots

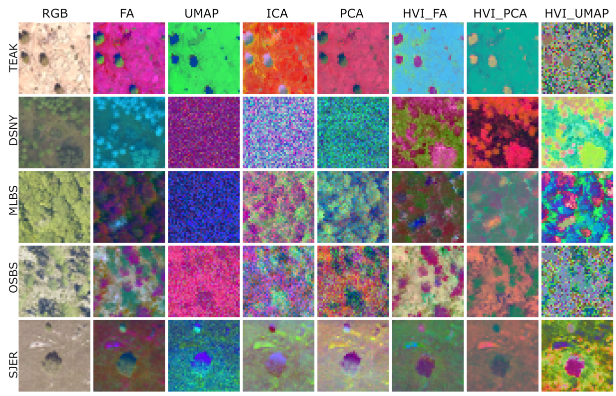

Figure 3. Dimensionality Reduction results using semi-global approach of five example plots

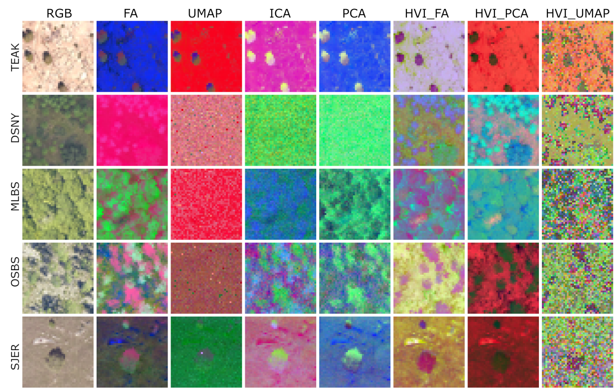

Figure 4. Dimensionality reduction results using selected global approach of five example plots

The evaluation process is limited to bounding boxes. Reference data is not given in the benchmark as detailed tree outlines, making much of the segmentation data redundant. These bounding boxes, created by a single observer, may be prone to human error, especially in dense forests. Additionally, SJER and TEAK account for over 57% of evaluation plots, while other sites have not enough annotations for a strong conclusion. The 1-meter resolution of the hyperspectral images fails to capture small trees, resulting in some bounding boxes being classified as false positives. Compared to a 2019 competition based on this hyperspectral benchmark dataset, this work achieved a lower mean IoU of 0.23, though it remains competitive - the top two teams scored 0.340 and 0.184, respectively (Marconi et al., 2019). These findings suggest the approach has potential and should be further explored, with recommendations for improvements provided in the next section.

6. Conclusion and outlook

6.1 Conclusion

This paper presented an application of hyperspectral dimensionality reduction (DR) methods to three channels for tree crown segmentation, assessed the segmentation performance of the Segment Anything Model (SAM), and proposed a filtering method for the segmented geometries. The effectiveness of the DR methods was found to be highly dependent on the forest characteristics of the sites and the method used. While some plots performed consistently well across all DR methods, others yielded unsatisfactory results for most methods. Notably, Factor Analysis and DR methods utilising HVIs proved to be the most effective and consistent, whereas other methods frequently produced noisy images. Upon visual inspection of the DR results, vegetation and non-vegetation could be effectively differentiated, though distinguishing between different vegetation types or individual trees remained challenging. Factor Analysis and HVI-based methods also performed best in differentiating between different trees in dense forest plots. The overall high performance of the HVI-based methods, also achievable through the multispectral imagery, indicates that the higher spectral content of hyperspectral was not sufficiently captured by the non-HVI methods to sufficiently improve ITC segmentation.

SAM's segmentation exhibited strong performance for isolated trees but encountered difficulties when segmenting trees in densely forested areas. The proposed geometry filtering method was effective at discarding non-vegetation objects, though it was less successful at removing non-tree vegetation, such as

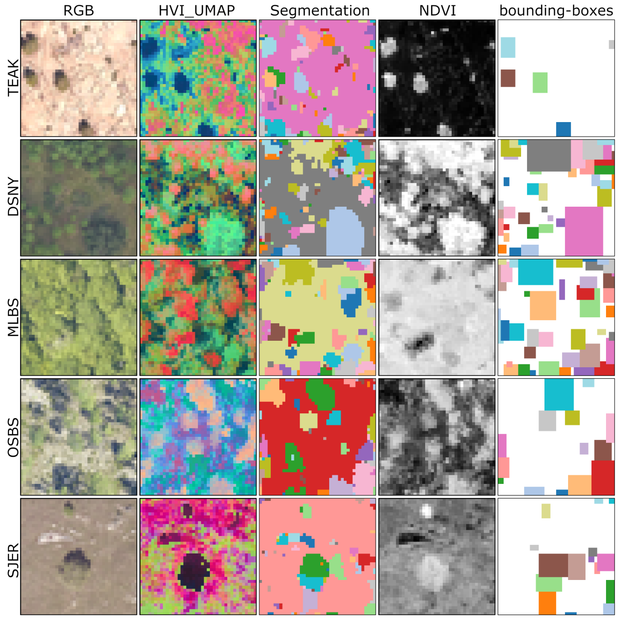

Figure 5. Results from HVI_UMAP method, illustrating the initial SAM segmentation results and the filtered segmented geometries, demonstrating oversegmentation

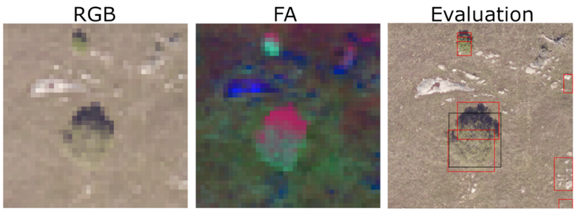

Figure 6. RGB image, FA dimensionality reduction result and evaluation results for a plot at SJER site, demonstrating the shadow issue leading to oversegmentation

bushes or grass. Evaluation results confirmed that reduced hyperspectral data resulted in better tree crown delineation compared to aerial RGB images with similar resolutions. However, none of the tested approaches achieved superior evaluation scores compared to the ID-Trees competition results (Graves et al., 2023), indicating that further improvements are necessary.

6.2 Outlook

Future work will explore additional DR methods to achieve more consistent results across diverse images. Fine-tuning existing methods like PCA, FA, and UMAP may enhance their performance. Employing supervised approaches, such as Linear Discriminant Analysis (LDA), could also improve differentiation between trees and other objects, though these require labeled data. Combining feature selection with feature extraction, such as selecting effective wavelengths for tree species classification (Hennessy et al., 2020) followed by DR methods like PCA or FA, presents another promising strategy similar to the HVI-based method discussed in this paper.

SAM proved effective for high-contrast segmentation but struggled with low-contrast objects, merging them into ”background geometries.” Adjusting SAM’s keyword arguments, as noted in the GeoSAM documentation (Wu and Osco, 2023), could improve recall, albeit at a potential cost to precision. The

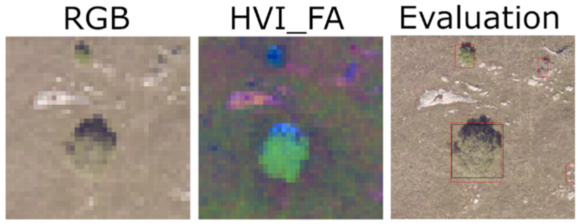

Figure 7. RGB image, HVI_FA dimensionality reduction result and evaluation results for a plot at SJER site, demonstrating the shadow issue being more successfully addressed in this method

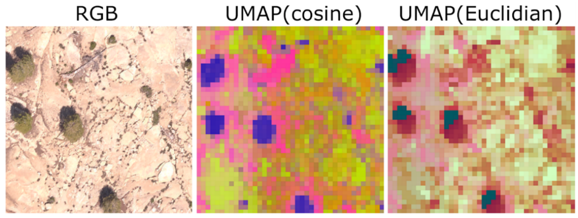

Figure 8. RGB image, UMAP Dimensionality Reduction result and evaluation results for a plot at SJER site, demonstrating the shadow issue being more successfully addressed with the UMAP-Euclidean method

newly released SAM 2, offering faster and more accurate segmentation, warrants investigation. Refining geometry selection within SAM parameters may further address under- or over-segmentation.

The dataset limitations noted in this study suggest that testing with higher-resolution datasets and alternative ground truth data, such as tree outlines instead of bounding boxes, would provide valuable insights into the DR and segmentation methods’ performance.

References

Graves, S. J., Marconi, S., Stewart, D., Harmon, I., Weinstein, B., Kanazawa, Y., Scholl, V. M., Joseph, M. B., McGlinchy, J., Browne, L., Sullivan, M. K., Estrada-Villegas, S., Wang, D. Z., Singh, A., Bohlman, S., Zare, A., White, E. P., 2023. Data science competition for cross-site individual tree species identification from airborne remote sensing data. *PeerJ*, 11, e16578. Publisher: PeerJ Inc.

Hennessy, A., Clarke, K., Lewis, M., 2020. Hyperspectral Classification of Plants: A Review of Waveband Selection Generalisability. *Remote Sensing*, 12(1), 113. Number: 1 Publisher: Multidisciplinary Digital Publishing Institute.

Hinton, G. E., Roweis, S., 2002. Stochastic Neighbor Embedding. *Advances in Neural Information Processing Systems*, 15, MIT Press.

Ke, Y., Quackenbush, L. J., 2011. A review of methods for automatic individual tree-crown detection and delineation from passive remote sensing. *International Journal of Remote Sensing*, 32(17), 4725–4747.

Keshava, N., 2004. Distance metrics and band selection in hyperspectral processing with applications to material identification and spectral libraries. *IEEE Transactions on Geoscience and Remote Sensing*, 42(7), 1552–1565. Conference Name: IEEE Transactions on Geoscience and Remote Sensing.

Khodr, J., Younes, R., 2011. Dimensionality reduction on hyperspectral images: A comparative review based on artificial datas. *2011 4th International Congress on Image and Signal Processing*, 4, 1875–1883.

Kirillov, A., Mintun, E., Ravi, N., Mao, H., Rolland, C., Gustafson, L., Xiao, T., Whitehead, S., Berg, A. C., Lo, W.-Y., Doll´ ar, P., Girshick, R., 2023. Segment Anything. arXiv:2304.02643 [cs].

Lennon, M., Mercier, G., Mouchot, M., Hubert-Moy, L., 2001. Independent component analysis as a tool for the dimensionality reduction and the representation of hyperspectral images. *IGARSS 2001. Scanning the Present and Resolving the Future. Proceedings. IEEE 2001 International Geoscience and Remote Sensing Symposium (Cat. No.01CH37217)*, 6, 2893–2895 vol.6.

Li, H., Cui, J., Zhang, X., Han, Y., Cao, L., 2022. Dimensionality Reduction and Classification of Hyperspectral Remote Sensing Image Feature Extraction. *Remote Sensing*, 14(18), 4579. Number: 18 Publisher: Multidisciplinary Digital Publishing Institute.

Marconi, S., Graves, S. J., Gong, D., Nia, M. S., Bras, M. L., Dorr, B. J., Fontana, P., Gearhart, J., Greenberg, C., Harris, D. J., Kumar, S. A., Nishant, A., Prarabdh, J., Rege, S. U., Bohlman, S. A., White, E. P., Wang, D. Z., 2019. A data science challenge for converting airborne remote sensing data into ecological information. *PeerJ*, 6, e5843. Publisher: PeerJ Inc.

Maschler, J., Atzberger, C., Immitzer, M., 2018. Individual Tree Crown Segmentation and Classification of 13 Tree Species Using Airborne Hyperspectral Data. *Remote Sensing*, 10(8), 1218. Number: 8 Publisher: Multidisciplinary Digital Publishing Institute.

McInnes, L., Healy, J., Melville, J., 2020. UMAP: Uniform Manifold Approximation and Projection for Dimension Reduction. arXiv:1802.03426 [cs, stat].

Minaee, S., Boykov, Y., Porikli, F., Plaza, A., Kehtarnavaz, N., Terzopoulos, D., 2022. Image Segmentation Using Deep Learning: A Survey. *IEEE Transactions on Pattern Analysis and Machine Intelligence*, 44(7), 3523-3542.

Osco, L. P., Wu, Q., De Lemos, E. L., Gonçalves, W. N., Ramos, A. P. M., Li, J., Marcato, J., 2023. The Segment Anything Model (SAM) for remote sensing applications: From zero to one shot. *International Journal of Applied Earth Observation and Geoinformation*, 124, 103540.

Pedregosa, F., Varoquaux, G., Gramfort, A., Michel, V., Thirion, B., Grisel, O., Blondel, M., Prettenhofer, P., Weiss, R., Dubourg, V. et al., 2011. Scikit-learn: Machine learning in Python. *the Journal of machine Learning research*, 12, 2825–2830.

Powell, W. B., 2007. *Approximate Dynamic Programming: Solving the Curses of Dimensionality*. John Wiley & Sons. Google-Books-ID: WWWDkd65TdYC.

Ruiz Hidalgo, D., Bacca Cortés, B., Caicedo Bravo, E., 2021. Dimensionality reduction of hyperspectral images of vegetation and crops based on self-organized maps. *Information Processing in Agriculture*, 8(2), 310–327.

Saeed, N., Nam, H., Haq, M. I. U., Muhammad Saqib, D. B., 2018. A Survey on Multidimensional Scaling. *ACM Comput. Surv.*, 51(3), 47:1–47:25.

Silva, V., Tenenbaum, J., 2002. Global Versus Local Methods in Nonlinear Dimensionality Reduction. *Advances in Neural Information Processing Systems*, 15, MIT Press.

Steier, J., Goebel, M., Iwaszczuk, D., 2024. Is Your Training Data Really Ground Truth? A Quality Assessment of Manual Annotation for Individual Tree Crown Delineation. *Remote Sensing*, 16(15), 2786.

van der Maaten, L., Postma, E., Herik, H., 2007. Dimensionality Reduction: A Comparative Review. *Journal of Machine Learning Research - JMLR*, 10.

Weinstein, B. G., Graves, S. J., Marconi, S., Singh, A., Zare, A., Stewart, D., Bohlman, S. A., White, E. P., 2020. A benchmark dataset for individual tree crown delineation in co-registered airborne RGB, LiDAR and hyperspectral imagery from the National Ecological Observation Network. Pages: 2020.11.16.385088 Section: New Results.

Wen, J., Fowler, J. E., He, M., Zhao, Y.-Q., Deng, C., Menon, V., 2016. Orthogonal Nonnegative Matrix Factorization Combining Multiple Features for Spectral–Spatial Dimensionality Reduction of Hyperspectral Imagery. *IEEE Transactions on Geoscience and Remote Sensing*, 54(7), 4272– 4286. Conference Name: IEEE Transactions on Geoscience and Remote Sensing.

Wu, Q., Osco, L. P., 2023. samgeo: A Python package for segmenting geospatial datawith the Segment Anything Model (SAM). *Journal of Open Source Software*, 8(89), 5663.

Xi, X., Xia, K., Yang, Y., Du, X., Feng, H., 2021. Evaluation of dimensionality reduction methods for individual tree crown delineation using instance segmentation network and UAV multispectral imagery in urban forest. *Computers and Electronics in Agriculture*, 191, 106506.

Xue, J., Su, B., 2017. Significant Remote Sensing Vegetation Indices: A Review of Developments and Applications. *Journal of Sensors*, 2017(1), 1353691. _eprint: https://onlinelibrary.wiley.com/doi/pdf/10.1155/2017/1353691.

Yong, A. G., Pearce, S., 2013. A Beginner’s Guide to Factor Analysis: Focusing on Exploratory Factor Analysis. *Tutorials in Quantitative Methods for Psychology*, 9(2), 79–94.